In situ observation and numerical calculations of the evolution of metallic foams

2006 J. Phys.: Condens. Matter 18 6493

(http://iopscience.iop.org/0953-8984/18/28/005)

INSTITUTE OF PHYSICS PUBLISHING JOURNAL OF PHYSICS: CONDENSED MATTER

J. Phys.: Condens. Matter **18** (2006) 6493–6506 doi:10.1088/0953-8984/18/28/005

In situ observation and numerical calculations of the evolution of metallic foams

O Brunke[1] **and S Odenbach**

TU Dresden, Professur für Magnetofluiddynamik, 01062 Dresden, Germany

E-mail: Oliver.Brunke@desy.de

Received 21 April 2006, in final form 29 May 2006
Published 28 June 2006
Online at stacks.iop.org/JPhysCM/18/6493

Abstract

During the past two decades the drainage behaviour and temporal evolution of aqueous foams has been subjected to intensive research activities. For the *in situ* monitoring of liquid metallic foams, it is not possible to use the established drainage observation methods employed for aqueous foams. The generally high melting point and conductivity as well as the opaque nature of these systems require the use of high temperature furnaces in combination with radiography techniques based on x-rays or neutrons. Due to these experimental difficulties, the data from a direct *in situ* observation of the material redistribution in liquid metallic foams has not been tested quantitatively with numerical solutions from any of the existing drainage models. In two recent studies the density profiles of solidified aluminium foam columns at different stages of the ageing process have been compared with corresponding numerical solutions of the Plateau channel-dominated drainage equation. However, due to the stochastic nature of the foam structure and its development, it was not possible to achieve a reliable quantitative comparison. In our paper we will show a direct quantitative comparison between experimental observations performed by means of x-ray radioscopy and numerical solutions of an adapted version of the channel-dominated drainage equation. Our results indicate that this theory can in principle be used to predict the temporal evolution during the ageing of metallic foams. By incorporating coalescence effects into the numerical description it can be shown that the material redistribution strongly depends upon the rate at which the pore structure evolves. This is in good agreement with our experimental observations.

(Some figures in this article are in colour only in the electronic version)

[1] Present address: HASYLAB at DESY, Builduing 25c, Notkestraße 85, 22067 Hamburg, Germany.

1. Introduction

Over the last fifteen years, metallic foams based on aluminium have become of significant interest for basic research as well as industrial applications because of their attractive physical properties. The favourable stiffness-to-weight ratio and excellent energy absorption capabilities of these systems make them very competitive with their more familiar polyurethane counterparts. For example, metallic foams combine these properties with low flammability and easy recyclability which makes them suitable for light weight applications in the automotive industry [1, 2].

The first patents for the processing of metallic foams appeared more than half a century ago. The multitude of different production routes which have been developed up to now [3–6] can be roughly divided into one or the other of the two major groups of processing, i.e. powder metallurgical or melt metallurgical. For almost any production route the genesis of the foam, e.g. the expansion of the gas bubbles, appears within the liquid state during which the structure is in a dynamic rather than a static state.

A deeper understanding of the physical processes which are involved in the growth and decay of liquid metallic foams and the incorporated changes of their structure has developed within the last ten years due to an increase in the number of experimental and theoretical studies. Three-dimensional (3D) image analysis of x-ray tomographic observations of solidified foam samples after different processing times show properties of the early stages during the bubble growth phase [7, 8] as well as the changes of the cell and cell-wall structure [9] during the ageing of aluminium foams produced by powder-metallurgical routes. The temporal development of the structure of liquid metallic foams and the redistribution of material can be directly observed by means of synchrotron based and neutron radioscopy [10–13], but no quantitative evaluation and comparison with numerical calculations are available at this time.

The liquid redistribution in foams is dependent on the properties of the liquid–gas interface which defines the dominating dissipation effect for the flow and is mathematically be described by different types of a single nonlinear differential equation. Comprehensive studies of the foam drainage equation (FDE) for the different dissipation mechanisms have been performed by Koehler *et al* [14] and Neethling *et al* [15]. For the case of an infinite surface viscosity at the interface, e.g. non-slip boundary conditions, the flow in aqueous foams can successfully be predicted by means of the channel-dominated FDE, [16, 17]. For the description of the liquid behaviour in metallic foams Gergely and Clyne [18] recently published a numerical study based on the channel-dominated FDE, including both the liquid in the network of the Plateau borders (PBs) and also inside the films. In this study a comparison of simulation results with some experimental drainage data of metallic foams showed reasonable agreement.

By comparing numerical solutions of the FDE with the density profiles of metallic foam columns solidified after different processing times, the authors of the present study show that the results given by the FDE underestimate the duration of the drainage process, i.e. the material redistribution, of metallic foams by from one to two orders of magnitude [19]. The reason for this discrepancy is partly due to the high liquid content, ϕ_l, of between 0.15 and 0.2 for these systems. This results in a large cross-sectional area of the PB channels for the simulation. In addition, the viscosity of the precursor melt is rather low ($\eta \approx 1$ mPa s). Therefore, in order to attain the slow experimentally observed redistribution of liquid, (where the equilibrium profile was established after about 5 min), an effective viscosity η^* was introduced. The measured bulk viscosity of the precursor material was increased by one to two orders of magnitude. The study showed that the FDE can be used as the starting point for a numerical description of the ageing processes in metallic foams. But it also revealed that the statistical nature of the foam dynamics demand that an *in situ* observation of the system in the liquid state by means

of radioscopic imaging is required in order to provide an ongoing monitoring of the changes of the foam structure.

Within the present work a small scale experiment for the observation of liquid aluminium foam columns by means of x-ray radioscopy is introduced. The observations show that the liquid redistribution during the foam ageing is strongly influenced by the coalescence of bubbles. Quantitative information on the evolution of the bubble size due to coalescence events has been obtained by means of tomographic examinations of solidified foam samples which have been frozen at different points of their temporal development. Finally, the measured drainage behaviour has been compared to solutions of a modified one-dimensional (1D) channel-dominated drainage equation. The comparison indicates that the model can describe the timescale of the measured liquid redistribution when using the known literature values for the viscosity and surface tension of the bulk precursor material.

2. Experimental setups and procedures

2.1. Foam precursor preparation

Foam samples for the present study have been produced by means of the powder-metallurgical (PM) process which was developed by the Fraunhofer institute IFAM in Bremen [5, 20]. Using this route, the preparation of the precursor material is carried out by mixing together the metal powder and blowing agent powder. The production of the foam is then carried out in a separate step. The precursor material was manufactured at Schunk Sintermetalltechnik GmbH (Gießen, Germany). In the production of the precursor, aluminium powder (grain radius $r < 160\ \mu$m) was mixed with silicon powder ($r < 160\ \mu$m) in a weight ratio of 93:7, resulting in an alloy comparable to commercial A356 (AlSi7). Subsequently, 0.6 wt% of the blowing agent TiH_2 is added. To finally obtain the dense precursor material, this mixture is compacted to a final density of about 99.5% of the bulk value by extrusion moulding at about 350 °C. The foam is now ready to be made by the melting of the precursor in a furnace at a temperature where the blowing agent releases its hydrogen and generates a foam-like melt. In order to conserve the porous foam structure the sample is finally cooled down below the melting point.

2.2. Drainage furnace and x-ray system

The experimental system developed for the *in situ* drainage observation consists of two major parts: (i) the furnace system equipped with two rotational axes for the metallic foam generation and (ii) a modular table-top x-ray system for radioscopic and tomographic examinations.

2.2.1. The drainage furnace. In order generate a set of controlled states for the experimental analysis of the ageing processes of a foam it is desirable to separate the growth and expansion phase from the decay phase. It is also preferable that the foam samples have a reproducible and homogenous initial density profile. Although the foam production by means of the powder-metallurgical method described in the previous section is simpler, it has the disadvantage that there is no clear separation between the foam growth phase and the ageing phase, i.e. some drainage of the liquid has already occurred during the expansion phase.

A solution to this problem has been realized with the furnace environment presented in figure 1. Similarly to the method described by Brunke *et al* [19], it allows for a rotation of the foam sample around two axes. The separation of the two phases is achieved as follows: the cylindrical foam sample is positioned horizontally during the expansion phase and vertically during the observation of the ageing and collapse phase. For this purpose, the whole furnace

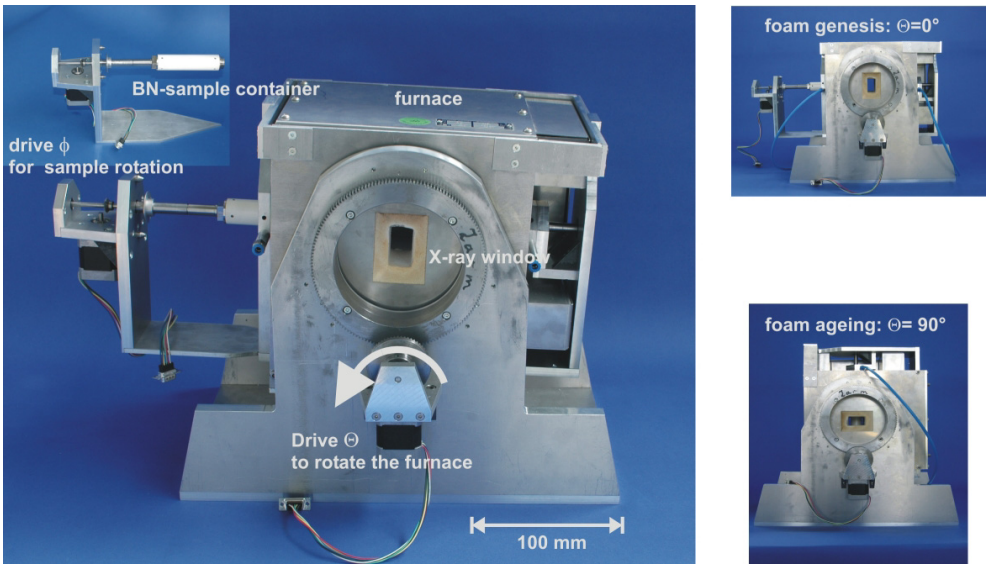

Figure 1. The furnace system developed for the *in situ* observation of the ageing of metallic foams.

can be rotated by 90° around the Θ axis shown in figure 1. Furthermore, it has been shown by Brunke *et al* [21] that by employing a slow axial ϕ rotation during the expansion phase it is possible to reduce the radial inhomogeneity within the foam cylinder.

For the optimum observation of the liquid metallic foams by means of x-rays, it is important to minimize the absorption of the photon intensity due to the sample container and the furnace system. The latter is therefore equipped with two view-ports with an area of 35 × 80 mm^2, which are covered by standard aluminium foil in order to reduce the loss of heat. The cylindrical foam samples with 60 mm length and 20 mm diameter are grown within a crucible made from boron nitride (BN) which combines a high transparency for x-rays with a good chemical resistance against the corrosive effects of liquid aluminium.

2.2.2. The x-ray system. An image of the x-ray setup is shown in figure 2(a). It comprises a 50 W (50 kV, 1 mA) x-ray tube with a spot size of about 40 μm diameter and the x-ray detector. There is also either an adjustable sample table for mounting the furnace systems or a rotational axis for tomography measurements. The latter features a 100 × 100 mm^2 phosphor screen which is coupled to a cooled low noise 1024 × 1024 CCD detector (type: back-thinned Marconi 47-10) by means of a macro lens system. Depending on the required spatial resolution, the maximum image frequency lies between ≈0.1 Hz for the readout of the whole CCD at 4 s exposure time and ≈3 Hz for a 125 × 125 pixel image (binning factor 8) at 50 ms exposure time. The radioscopic image in figure 2(b) shows a 256 × 256 pixel image (binning factor 4) of a completely expanded aluminium foam with a pixel size of 300 μm recorded at a frame rate of about 1 Hz and 200 ms exposure time.

2.3. Observing the foaming process

A typical example of the evolution of the foam structure during the growth phase and the decay phase at a fixed process temperature of 750 °C is illustrated in the image sequence of figure 3.

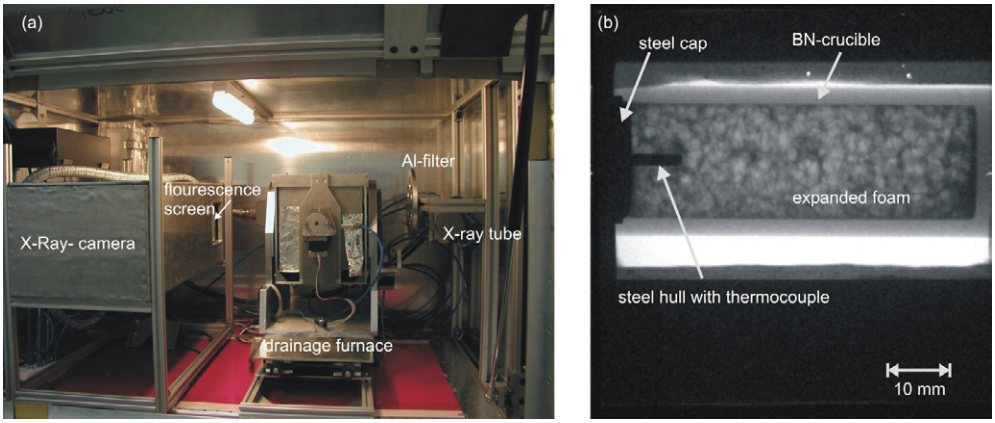

Figure 2. X-ray setup with integrated furnace for the *in situ* observation of liquid metallic foams (a) and radioscopic image of a completely expanded Al foam sample (b).

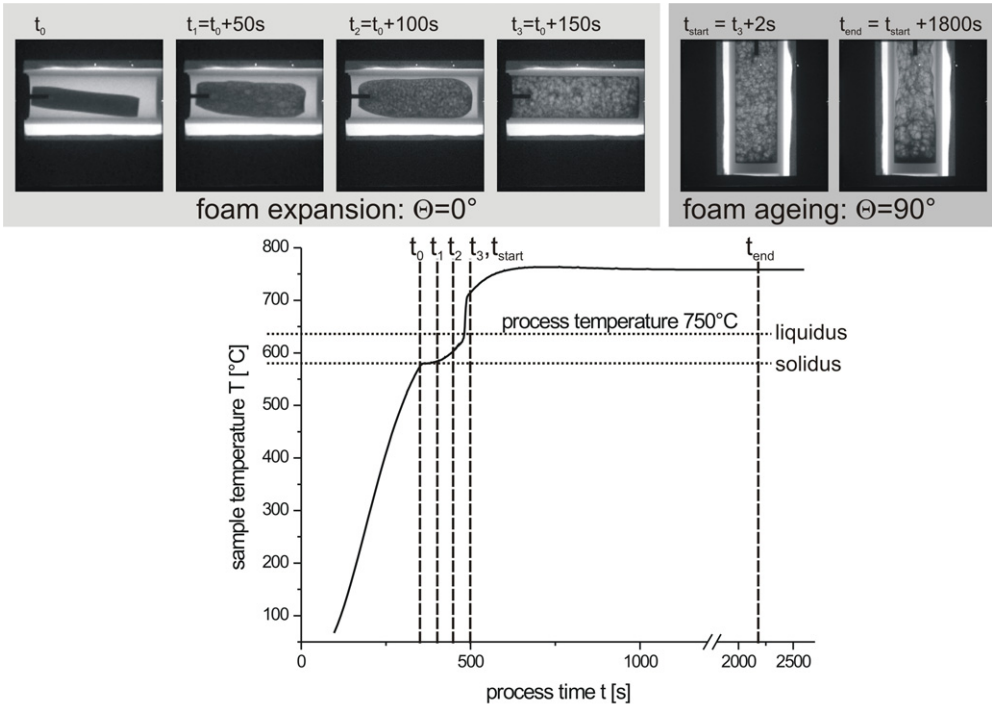

Figure 3. Radioscopic sequence of the foam expansion and decay at a 750 °C process temperature. The graph shows the corresponding run of the sample temperature.

The evolution of the foam is discussed in terms of a growth phase (i) and a decay or ageing phase (ii).

In the beginning of phase (i) the precursor which is axially centred within the BN sample container is transferred into the preheated furnace which allows a fast heat-up rate of 1.5 K s^{-1}. A fast heating of the sample is preferred in order to minimize the time between the decomposition temperature of the blowing agent (400 °C) [22] and the melting of the alloy.

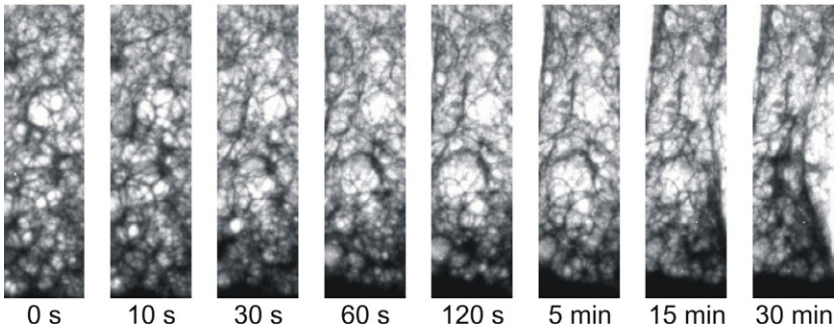

Figure 4. Redistribution of liquid in an aluminium foam column at a 750 °C process temperature.

Due to the elution of gas from the sample during this phase, a slower heating rate leads to an undesired amount of unused gas and thus a smaller expansion of the foam [23]. The size of the precursor sample was chosen such that the foam sample completely filled the container at its maximum volume expansion of about 500%. The graph underneath the x-ray image sequence shows the corresponding run of the sample temperature. It is used to control the foaming process in order to achieve reproducible experimental conditions for all samples. As soon as the liquidus (630 °C for AlSi7) of the alloy is reached at t_0, both an axial rotation with $\dot{\phi} \approx 0.1$ Hz and the recording of the radioscopic images are initiated. For a process temperature of 750 °C the expansion of the foam reaches its maximum, typically after about 150 s (t_3). The axial rotation is completed and the sample is brought into a vertical position within less than 2 s. This defines the starting point t_{start} of phase (ii). The ageing process is now observed for 30–60 min until the final stage of the sample evolution has been reached.

3. Results

3.1. The redistribution of liquid

Following the procedure described in the previous section, the ageing phase of aluminium foam columns has been observed in order to gain information about the redistribution of the liquid which is a major source of structural inhomogeneities within solidified foams.

The image sequence presented in figure 4 shows typical stages of the evolution of a foam column at a 750 °C process temperature within an observation period of 30 min. During the first 30 s the cellular structure of the foam evolves very quickly due mainly to the coalescence events. After about 60 s the formation of a liquid pool at the bottom of the column can be observed. Within less than 5 min the process reaches an equilibrium-like state. Apart from slight deformations of the outer boundary, the foam sample is stable during the radioscopic imaging of about 30 min.

For a systematic analysis and a direct comparison to a numerical solution of the drainage equation, it is useful to perform a reduction of the image data. This procedure comprises two steps.

(1) The intensity values of the absorption images are converted to absolute density values. This is a non-trivial task due to the polychromatic characteristic of the x-ray source and an inhomogeneous sensitivity of the detector system. Therefore it was necessary to measure the absorption behaviour of appropriate calibration objects with known density and thickness and with the same projected area as the foam samples. By measuring

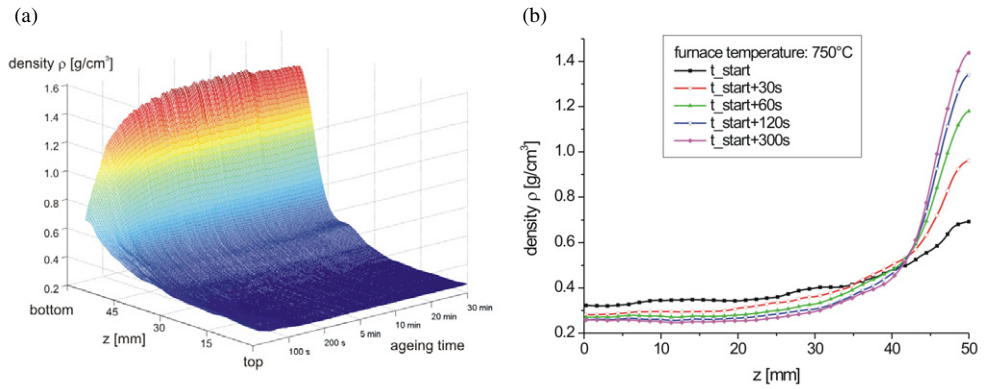

Figure 5. The surface plot (a) shows the average evolution of seven aluminium foam columns at a 750 °C process temperature. A closer look to the first 300 s of the process reveals that most of the liquid has already been redistributed within the first 120 s after rotating the samples to the vertical position.

the absorption characteristic for these objects at different thicknesses it was possible to determine the two-dimensional (2D) density maps from the intensity images. It is then straightforward to generate a temporal series of 1D density profiles by calculating the mean value of each row of the 2D density maps.

(2) In order to account for the statistical fluctuations of the foaming process, the experiment was repeated seven times under identical conditions with respect to the process temperature and precursor material. The calculation of the average temporal evolution of the 1D density profile for these seven samples results in the surface plot shown in figure 5(a). Here, the average density of the seven samples is plotted as a function of time and vertical position within the foam column. Figure 5(b) shows the development of the vertical density profiles within the first 300 s of the process. Clearly most of the liquid has been redistributed already after about 120 s, and only minor changes can be observed in the following time.

3.2. Evolution of the bubble size

During the expansion and ageing of metallic foams, the cellular structure is subjected to strong changes, as seen in the x-ray observations of this work and in previous studies [11, 13, 24]. The growth of the mean cell size in metallic foams is dominated by coalescence effects, i.e. the merging of adjacent foam bubbles due to the thinning and rupture of their separating walls. In contrast to most aqueous foams, the cell walls in metal foams are less stable to thinning due to the gravity and capillary driven drainage. Coarsening, i.e. the increase of the mean cell size due to the pressure difference in adjacent bubbles, plays practically no role due to the relative high thickness of the walls. In the case of aluminium based foams a wall thickness of between 10 and 100 μm has been reported [13, 25–27], which form an effective barrier against gas diffusion.

By means of suitable image analysis techniques it is possible to determine cell wall rupture events from the x-ray sequences [28, 29]. While the analysis of 2D x-ray absorption images offers a good temporal resolution to determine the coalescence rate, it is not possible to directly obtain quantitative information about the mean bubble size or its distribution. A common method for the 3D analysis of the foam structure is x-ray tomography [8, 26, 30–32]. The long scanning time from several tens of minutes to hours for one tomographic scan usually does not allow the foam samples to be observed in the liquid state. However, recent developments

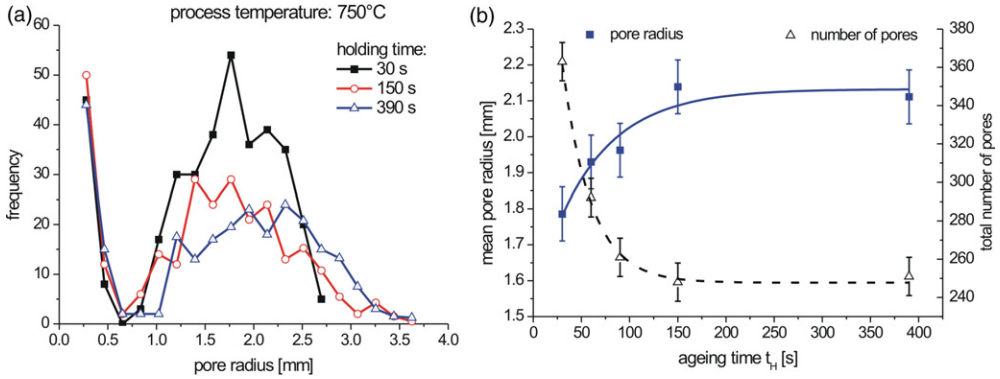

Figure 6. (a) Development of the pore size distributions at a 750 °C process temperature given by the analysis of tomographic datasets of solidified foam samples after different ageing times. (b) Evolution of the mean pore size and the total number of pores within the first 400 s of the process.

at synchrotron sources have shown that in principle it is possible to analyse liquid foam samples [33] as long as the scanning time is short in comparison to the changes of the sample structure during the scan.

Within the present work, the growth of the pore structure has been determined from tomographic scans of solidified foam samples by means of the same 3D image analysis methods that have been used in [25]. By quenching the samples within about 10 s after a predefined foaming time it was possible to conserve the structure of the respective stage of the ageing process. The foaming, which was performed at a process temperature of 750 °C, was stopped after five different times between 30 and 400 s. For each of these points, three samples were produced under identical conditions in order to account for statistical fluctuations. Tomographic scans at a spatial resolution of about 100 μm were performed by means of a modified version of the x-ray setup presented in section 2.

In figure 6(a) the bubble size distributions determined by the image analysis of the tomographic datasets of foam samples solidified after 30, 150 and 390 s are shown. The behaviour of the mean pore radius as well as the total number of pores as a function of process time is given in figure 6(b). After about 150 s, the mean pore radius becomes stable and the coalescence stops. This saturation behaviour is in good accordance with the point in time at which the liquid redistribution reaches its equilibrium as indicated by the radioscopic observations.

A similar correlation between the bubble size growth due to coarsening and the liquid redistribution is well known for water based foams [34]: larger pores lead to wider Plateau channels and therefore to an increased drainage speed. If the timescale for the coarsening is smaller than the drainage timescale, a strong coupling between the bubble size evolution and the drainage behaviour may be observed [35].

The results of the radioscopic and tomographic study for the ageing of metallic foams now clearly indicate a similar coupling behaviour. The redistribution of material in such foams is strongly influenced by the coalescence of cell walls.

4. Assumptions for the drainage model

A major goal of this study has been to verify whether it is possible to describe the experimentally observed material redistribution by means of the channel-dominated FDE. This

equation is a nonlinear partial differential equation for the liquid content ϕ_l or the PB area A_{PB} as a function of time and space. Under the assumption of a time-dependent number N (i.e. size) of foam cells the 1D form of the FDE reads as follows [36]:

$$\frac{\partial \phi_l}{\partial t} + N^{-1}\frac{\partial N}{\partial t}\phi_l + \frac{1}{3f\eta}\frac{\partial}{\partial z}\left(\rho g \phi_l^2 - \frac{C\gamma}{2}\sqrt{\phi_l}\frac{\partial \phi_l}{\partial z}\right) = 0. \tag{1}$$

The quantities f and C are well known parameters [37], with $f \approx 49$ describing the viscous drag in a channel having the concave triangular shape of an ideal PB cross-section. Additional parameters are the density ρ, viscosity η and surface tension γ of the liquid of the foam. Numerical solutions of this equation have been calculated by means of an explicit finite difference method with a constant step-size.

As mentioned above, a first comparison for AlSi7 foams presented in [19] with a constant pore size N revealed that the redistribution rate obtained from equation (1) overestimates the experimental observations by at least one order of magnitude. Also the influence of the oxide content of the precursor material on the bulk viscosity was analysed experimentally within this work. In comparison with the value for pure AlSi7 at 700 °C ($\eta_{precur} = 1.2$ mPa s), the viscosity of the precursor material which contained 0.6 wt% of oxides increased by a factor of about 1.4. However, a reasonable agreement between the measurements and the numerical results of the redistribution rate could only be achieved by a much stronger increase of the viscosity value in the numerical calculation. In [19] a factor of ten was employed to slow down the simulated material redistribution rate.

This approach would clearly also be suitable to reproduce the general timescale of the experimental redistribution behaviour shown in figure 5. But it can be shown that in this case at the equilibrium density profile, the relative liquid content at the top of the foam column decreases by more than 90% from the initial value in the case of the simulation, whereas for all experimental observations this decrease was 40% or less. An alternative approach has therefore been made for the current numerical simulations to address this discrepancy with a modification that can be implemented by introducing some assumptions based on a simplified interpretation of some experimental observations of the foaming process.

The evolution of the foam structure is subjected to major changes which are driven by pore coalescence and drainage. However, a very stable foam skeleton is observed to remain at the end of this redistribution process, (cf the last three images of the sequence in figure 4), which is stable for hours and degrades only slowly. This experimental evidence strongly suggests that not all the material of the foam column contributes to the drainage flow. Further support for this idea can be found in a recent publication of Körner *et al* [38] on the stabilization mechanism of Al foams produced by PM processes. Their results obtained by means of light microscopy and x-ray tomography indicate the formation of so-called agglomerate oxide particles with a very high effective volume content of up to 40%. However, the foam precursor material intrinsically contains only 0.4 wt% of aluminium oxide which originates from the oxide content of the aluminium powder used for the PM production route. Thus, the foaming process accounts for an increase of the effective oxide volume content of about two orders of magnitude. According to the experimental observations of Körner the agglomerate oxide particles exhibit a solid-like behaviour. As a first approximation for the simplified numerical model it is assumed that the agglomerates can be treated as a solid phase which does not contribute to the drainage flow.

Therefore, with these observations providing a background to the assumption that only a part of the overall material content can be redistributed and therefore effectively contribute to the drainage flow, the FDE has been solved using a modified form of the effective liquid content:

$$\tilde{\phi}_l = k\phi_l \qquad \text{with } 0 < k < 1. \tag{2}$$

This decrease in the effective liquid content then results in a smaller cross-sectional area of the PB and thus gives rise to a reduced flow speed in the simulation.

In order to be able to implement this modification, a suitable value must be attributed to the factor k. For this purpose an additional very simple assumption has been introduced into the simulation that relates a linear growth of the volume content of the agglomerate with an increase of the intrinsic oxide content of the precursor material. Clearly, this approach can only be regarded as an expedient measure to facilitate an initial numerical solution and investigate the behaviour of the modified FDE. In comparison with Körner *et al*, the oxide content of the precursor material used within the present work is roughly a factor of 1.5 higher. Therefore, a factor of $k = 0.4$, which is equivalent to an effective agglomerate particle content of 60%, has been selected for the simulation.

Finally, in order to account for the coalescence effects, the experimentally determined decrease in the number of pores, $N(t)$, was included. For this purpose an exponential saturation function $N(t) = a + b\exp(-ct)$, describing the coalescence behaviour, was fitted to the dataset and this is shown by the solid line in figure 6(b). The resulting function was accordingly included into the numerical procedure for solving equation (1) above.

5. Comparison

The motivation for the introduction of the assumption of a reduced effective liquid content ($k < 1$) has been discussed above.

For a first comparison between the numerical simulation and the experimental results a modified model based on the FDE has been developed with the following features presumed.

(1) Only a part of the overall material volume contributes to the redistribution process.
(2) Agglomerate oxide particles do not contribute to the drainage flow.
(3) There is a linear growth of the volume content of the agglomerate with an increase of the intrinsic oxide content of the precursor material.

Based on these simple assumptions, a factor of $k = 0.4$, which is equivalent to an effective agglomerate particle content of 60%, has been selected for the simulation.

The surface plot in figure 7(a) shows the simulated evolution of the vertical density profile given by the numerical solution of the FDE (equation (1)) for the first 300 s of the ageing process. An effective liquid content with has been assumed for the simulation. A qualitative comparison with the experimental data obtained at a 750 °C process temperature (figure 7(b)) within that time period reveals a very similar appearance of the pattern. It furthermore shows a good agreement with the time-dependent behaviour of the density profiles. In both cases the material distribution reaches its equilibrium after about 200 s. While the time for the onset of the saturation in the experiment seems to be predicted accurately by the simulation, it overestimates the redistribution rate within the first 50 s of the process.

In order to provide a quantitative comparison between the simulated and the experimental datasets it is useful to determine the time-dependent behaviour of a global quantity. For this purpose the total amount of redistributed liquid ψ_l has been defined as

$$\psi_\mathrm{l} = \int_0^h \left[\varepsilon(\underbrace{\phi_\mathrm{l}(z,t_i) - \phi_\mathrm{l}(z,0)}_{a}) \cdot (\phi_\mathrm{l}(z,t_i) - \phi_\mathrm{l}(z,0)) \right] \mathrm{d}z \qquad \text{with}$$

$$\varepsilon(a) = \begin{cases} 1, & \phi_\mathrm{l}(a) \geqslant 0 \\ 0, & \phi_\mathrm{l}(a) < 0. \end{cases} \tag{3}$$

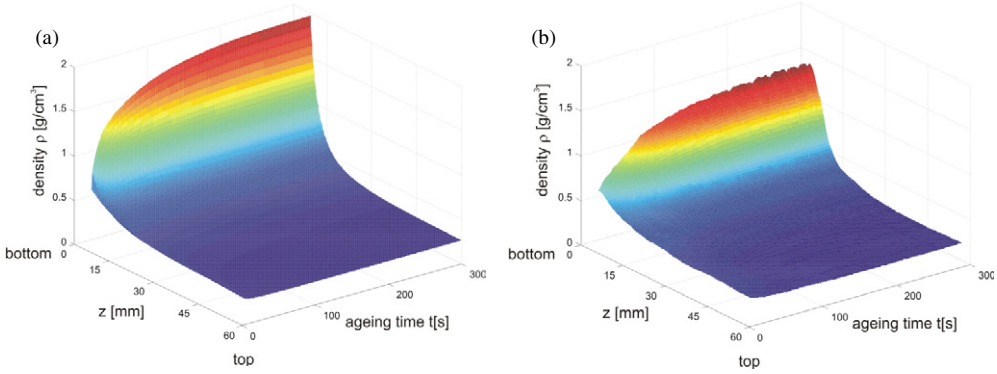

Figure 7. The surfaces plots shows the time-dependent vertical density profile resulting from the numerical solution of equation (1) (a) and the analysis of the x-ray observation at 750 °C process temperature (b), respectively.

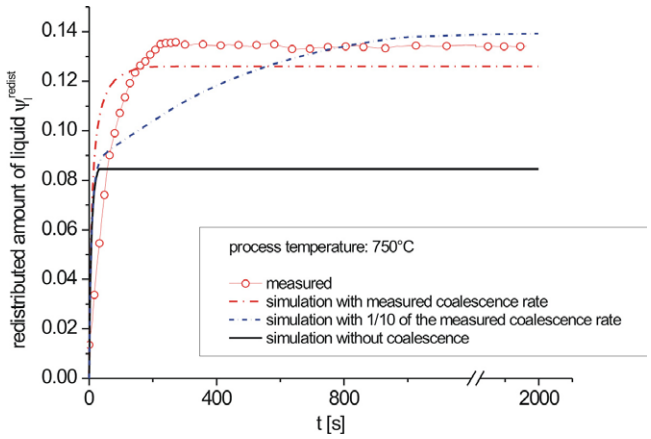

Figure 8. Total relative amount of redistributed liquid as a function of time. The open circles show the experimental data; the lines are simulated profiles for different coalescence rates.

Figure 8 shows the behaviour of ψ_l as function of the process time. The experimental data points are represented by open circles. Three different coalescence rates, indicated by the solid, dashed and dashed–dotted lines, have been chosen for the simulation by varying the parameter c in the empirical exponential coalescence function $N(t)$. The resulting curves of ψ_l for these three cases show the strong dependence of the material redistribution on the growth of the foam's cell size. From the experimentally determined coalescence rate, the dashed–dotted line, it can be seen that the simulation gives a good reproduction of the results evaluated from the radioscopic observations for the onset of saturation at 200 s and also for the value of ψ_l at equilibrium. The latter lies slightly below the experimental data and shows a deviation of less than 10%. If the simulated coalescence rate is slowed down to $1/10$ of the measured rate, the equilibrium value of ψ_l lies only about 5% above the experimental data, but it takes more than 1000 s until the saturation is reached. Finally, for the simulation with a vanishing coalescence rate, i.e. a constant pore size, and as is shown by the solid line in figure 8, the redistribution of liquid is seen to stop within 50 s, which is a factor of four faster than the experimental observation. Furthermore, the saturation value of ψ_l is seen to deviate from the experimental data by about 40%.

In conclusion, the simulated behaviour of ψ_l for different coalescence rates appears to confirm the statement made in section 3. The redistribution of liquid in metallic foams is strongly coupled to the evolution of the cellular structure. Therefore, an analysis of the pore coalescence effects is absolutely critical for the understanding of the drainage behaviour of these systems. By using a known value of the foam coalescence rate in the numerical solution of the 1D FDE, a good quantitative agreement between the simulated and experimental behaviour of ψ_l as shown in figure 8 can be achieved.

6. Summary and outlook

The ageing process of Al foams produced by a powder-metallurgical route has been studied in the liquid state. By means of a newly designed furnace system and a table-top x-ray setup it was possible to directly observe all phases of the foaming process using time-resolved radioscopic imaging. From the image sequences showing 2D projections of the foam structure during its ageing it was possible to evaluate the time-dependent development of the vertical density profile. X-ray tomography was used to determine the time dependence of the mean pore size. For this purpose the foaming process was interrupted by cooling the foams below their melting temperature at different times of the process. These measurements allowed the determination of an empirical function showing how the number of pores depended on the process time. The comparison between the timescale of the pore size evolution on the one hand and the material redistribution on the other indicates a strong coupling between these processes.

A simple 1D approach based on the channel-dominated foam drainage equation was used to simulate the redistribution of liquid within the foam samples. It could be shown that in principle it is possible to reproduce the experimental behaviour. However, in order to reach the relatively low redistribution rate observed in experiments, it was necessary to assume that only a fraction of the overall material within the metallic foam contributes to the flow. An indication for the feasibility of this assumption is the observation by Körner *et al* [38] that a high volume fraction of agglomerate oxide particles with solid-like behaviour has been found within powder-metallurgical Al foams. In addition, the experimentally measured empirical temporal function for the pore numbers was included in the simulation. Thus it was possible to quantitatively reproduce the global temporal behaviour of the observed density profile evolution at a 750 °C process temperature as well as the time after which the equilibrium state of the redistribution was reached. The saturation value for the total amount of liquid was reproduced satisfactorily by the simulation.

In conclusion, the channel-dominated FDE might therefore serve as a simple tool to predict the redistribution behaviour in liquid metal foams. As the next step it will be necessary to test the validity and accuracy of the model by comparing it to experimental situations with different coalescence rates, e.g. by a variation of the process temperature which has a major influence on the structural changes in metallic foams [23]. Further experiments employing a variation of the oxide content in the foam precursor material are suggested to achieve different concentrations of agglomerate particles. Hence, it would be possible to test whether their concentration influences the stability of the foam system and the material redistribution rate. These experiments could be used to show how the amount of effective liquid material in the foam system is affected by the oxide content of the precursor material.

In addition, the drainage behaviour of foams produced directly from the liquid state, like for example the ALCAN process, could be observed. By means of an improved x-ray system with a higher temporal and spatial resolution it will be possible to collected more detailed data on the material redistribution taking place in the first very fast phase of the ageing process. This will allow an experimental determination of the time-dependent variation of the liquid fraction

at different heights to be made with higher precision. Accordingly it will be possible to verify whether a Poisseuille-type flow dominates the drainage of metallic foams and thus whether the channel-dominated FDE is adequate or a more general approach as introduced by Koehler [14] or Neethling [15] will be needed.

Acknowledgments

This project was supported by ESA within the MAP programme A099-075. The authors want to express their gratitude to S J Cox for the help with the modelling and useful discussion as well as S Kroffke for supporting the development, construction and setup of the experimental systems.

References

[1] Banhart J 2005 Aluminium foams for lighter vehicles *Int. J. Vehicle Design* **37** 114–25
[2] Fuganti 2000 Al foam for automotive applications *Adv. Eng. Mater.* **2** 200–4
[3] Banhart J 2000 Manufacturing routes for metallic foams *J. Metals* **52** 22–7
[4] Banhart J 1999 Foam metal: the recipe *Europhys. News* **30** 17–20
[5] Yu C-J, Eifert H H, Banhart J and Baumeister J 1998 Metal foaming by a powder metallurgy method: production, properties and applications *Mater. Res. Innovation* **2** 181–8
[6] Ashby M F *et al* 1998 *Cellular Metals, A Design Guide* Cambridge University, Engineering Department
[7] Helfen L *et al* 2005 Investigation of pore initiation in metal foams by synchrotron-radiation tomography *Appl. Phys. Lett.* **86** (23)
[8] Helfen L *et al* 2002 Viewing the early stage of metal foam formation by computed tomography using synchrotron radiation *Adv. Eng. Mater.* **4** 808
[9] Brunke O, Odenbach S and Beckmann F 2004 Structural characterization of aluminium foams by means of micro computed tomography *SPIE: Developments in X-Ray Tomography IV* (Denver: SPIE Press)
[10] Stanzick H, Klenke J, Danilkin S and Banhart J 2002 Material flow in metal foams studied by neutron radioscopy *Appl. Phys.* A **74** S1118–20
[11] Stanzick H *et al* 2002 Process control in aluminum foam production using real-time x-ray radioscopy *Adv. Eng. Mater.* **4** 814–23
[12] Banhart J, Stanzick H, Helfen L, Baumbach T and Nijhof K 2001 Real-time x-ray investigation of aluminium foam sandwich production *Adv. Eng. Mater.* **3** 407–11
[13] Banhart J, Stanzick H, Helfen L and Baumbach T 2001 Metal foam evolution studied by synchrotron radioscopy *Appl. Phys. Lett.* **78** 1152–4
[14] Koehler S A, Hilgenfeldt S and Stone H A 2000 A generalized view of foam drainage: experiment and theory *Langmuir* **16** 6327–41
[15] Neethling S J 2002 A foam drainage equation generalised for all liquid contents *J. Phys.: Condens. Matter* **14** 331–42
[16] Weaire D, Hutzler S, Verbist G and Peters E 1997 A review of foam drainage *Adv. Chem. Phys.* **102** 315–38
[17] Verbist G, Weaire D and Kraynik A M 1996 The foam drainage equation *J. Phys.: Condens. Matter* **8** 3715–31
[18] Gergely V and Clyne T W 2004 Drainage in standing liquid metal foams: modelling and experimental observations *Acta Mater.* **52** 3047–58
[19] Brunke O, Hamann A, Cox S J and Odenbach S 2005 Experimental and numerical analysis of the drainage of aluminium foams *J. Phys.: Condens. Matter* **17** 1–10 (doi:10.1088/0953-8984/17)
[20] Kunze H D, Baumeister J, Banhart J and Weber M 1993 Möglichkeiten zur Herstellung von Bauteilen aus geschäumten Metallen *Pulvermetall. Wissenschaft Praxis-Band* **9** 330–47
[21] Brunke O and Odenbach S 2003 New experiments for influencing and observing the growth process of metallic foams *Cellular Metals—Manufacture, Properties, Applications* (Berlin: MIT-Verlag)
[22] Zeppelin F v, Hirscher M, Stanzick H and Banhart J 2003 Desorption of hydrogen from blowing agents used for foaming metals *Compos. Sci. Technol.* **63** 2293–2300
[23] Stanzick H 2003 Untersuchung der Bildung und des Kollapses von Metallschäumen *IFAM, Bremen Dissertation* (Berlin: Logos-Verlag)
[24] Stanzick H and Banhart J 2002 Material flow in metal foam studied by neutron radioscopy *Appl. Phys.* A **74** 1118–20

[25] Brunke O, Odenbach S and Beckmann F 2005 Quantitative methods for the analysis of synchrotron–muCT datasets of metallic foams *Eur. Phys. J. Appl. Phys.* **29** 73–81 (doi:10.1051/epjap: 2004203)
[26] Elmoutaouakkil A, S L, Maire E and Peix G 2002 2D and 3D characterization of metal foams using x-ray tomography *Adv. Eng. Mater.* **4** 803–7
[27] Rack A, Haibel A, Bütow A, Matijasevic B and Banhart J 2004 Characterization of metal foams with synchrotron-tomography and 3D image analysis *16th WCNDT 2004-World Conf. on NDT (Montreal)*
[28] García-Moreno F, Babcsán N and Banhart J 2005 x-ray radioscopy of liquid metalfoams: influence of heating profile, atmosphere and pressure *Colloids Surf.* A **263** 290–4
[29] García-Moreno F, Fromme M and Banhart J 2003 Real-time x-ray radioscopy on metallic foams using a compact micro-focus source *Cellular Metals—Manufacture, Properties, Applications* (Berlin: MIT-Verlag)
[30] Benouali A H, Froyen L, Delerue J F and Wevers M 2002 Mechanical analysis and microstructural characterisation of metal foams *Mater. Sci. Technol.-J. Mater. Sci. Technol.* **18** 489–94
[31] Maire E, Elmoutaouakkil A, Fazekas A and Salvo L 2003 *In situ* x-ray tomography measurements of deformation in cellular solids *MRS Bull.* **28** 284–9
[32] Maire E, Fazekas A, Salvo L, Dendievel R, Youssef S, Cloetens P and Letang J M 2003 x-ray tomography applied to the characterization of cellular materials. Related finite element modeling problems *Compos. Sci. Technol.* **63** 2431–43
[33] Michiel M D *et al* 2005 Fast microtomography using high energy synchrotron radiation *Rev. Sci. Instrum.* **76** 043702
[34] Hilgenfeldt S, Koehler S A and Stone H A 2001 Dynamics of coarsening foams: accelerated and self limiting drainage *Phys. Rev. Lett.* **86** 4704
[35] Langevin D and Saint-Jalmes A 2002 Time evolution of aqueous foams: drainage and coarsening *J. Phys.: Condens. Matter* **14** 9397–412
[36] Cox S J 2000 Applications and generalisation of the foam drainage equation *Proc. R. Soc.* A **456** 2441–64
[37] Weaire D and Hutzler S 1999 *The Physics of Foams* (Oxford: Clarendon)
[38] Körner C, Arnold M and Singer R F 2005 Metal foam stabilization by oxide network particles *Mater. Sci. Eng.* A **396** 28–40